

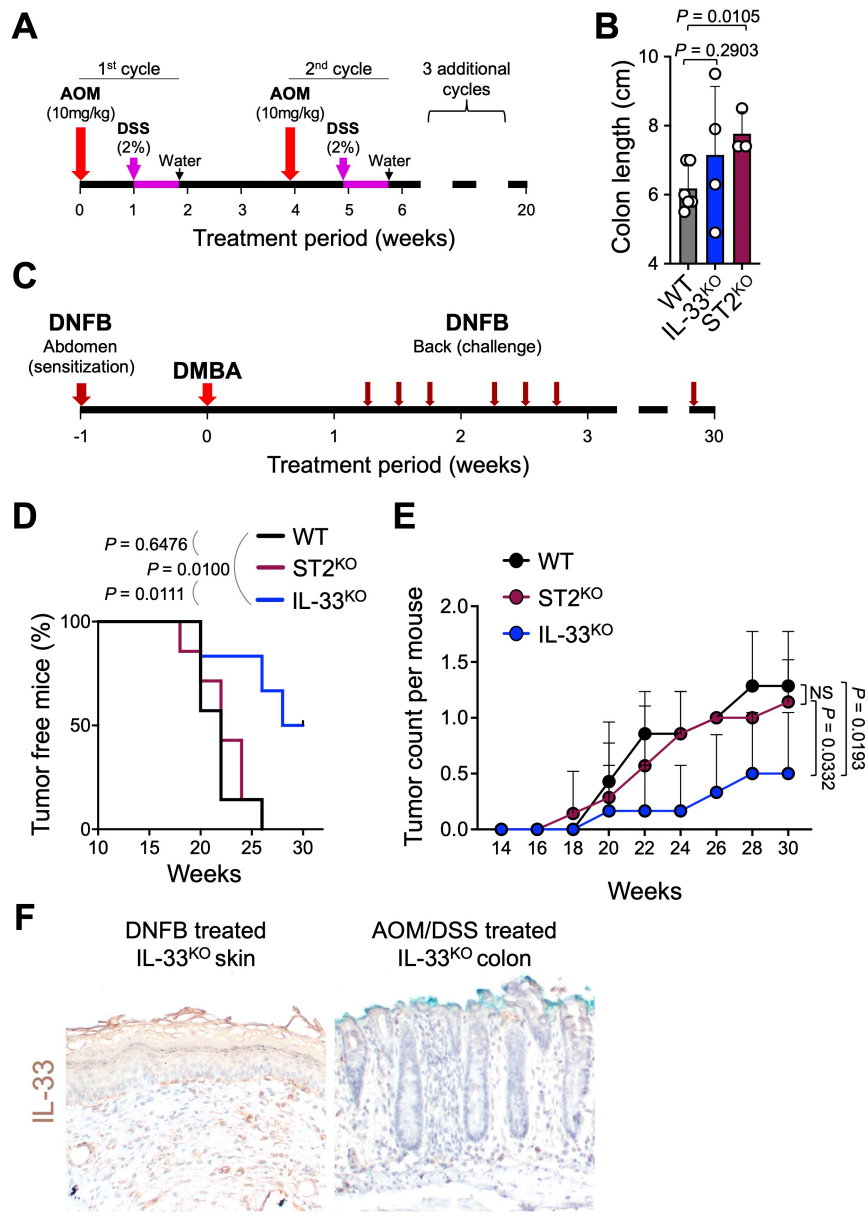
Appendix File

Table of Contents

Page 2 to 17: Appendix Figure S1 to S9

Page 18 to 25: Appendix Table S1 and S2

Appendix Figures



Appendix Fig S1. IL-33/ST2 impact on colorectal and skin carcinogenesis in chronic inflammation.

(A) Schematic diagram of colitis-induced colorectal carcinogenesis protocol in mice, consisting of five AOM/DSS treatment cycles over 20 weeks.

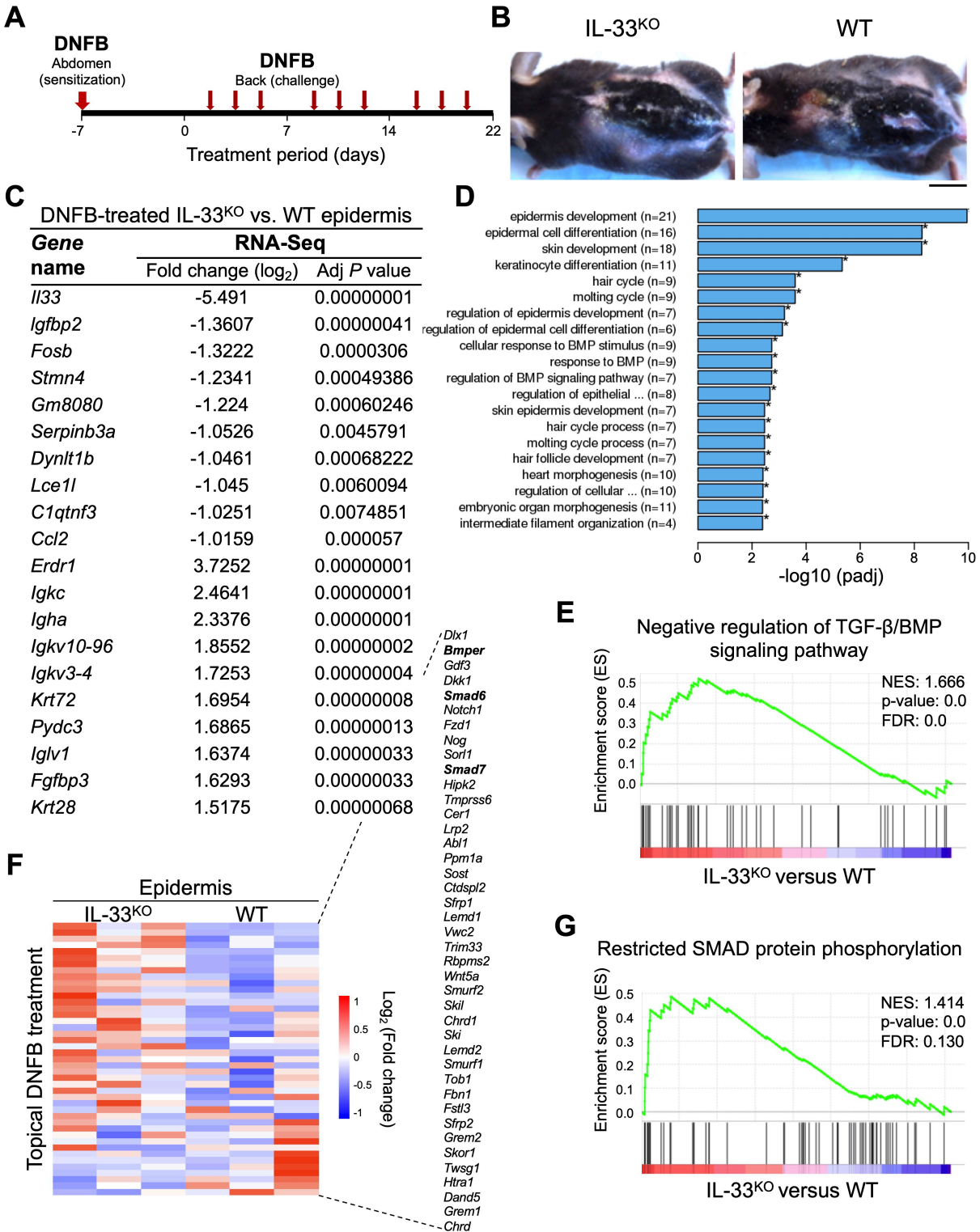
(B) Colon length measurement, from cecum to rectum, in WT (n=6), IL-33^{KO} (n=4) and ST2^{KO} (n=3) mice at the completion of the AOM/DSS carcinogenesis protocol.

(C) Experimental design for chronic inflammation-induced skin carcinogenesis consisting of an initial sensitization to DNFB allergen on the abdomen followed by treatment with a single dose of DMBA followed by DNFB challenges on the back skin three times a week for 29 weeks.

(D and E) Skin tumor outcome in WT (n=7), ST2^{KO} (n=7) and IL-33^{KO} (n=6) mice treated with DMBA/DNFB carcinogenesis protocol. (D) Time to tumor onset (log-rank test) and (E) the number of skin tumors over time.

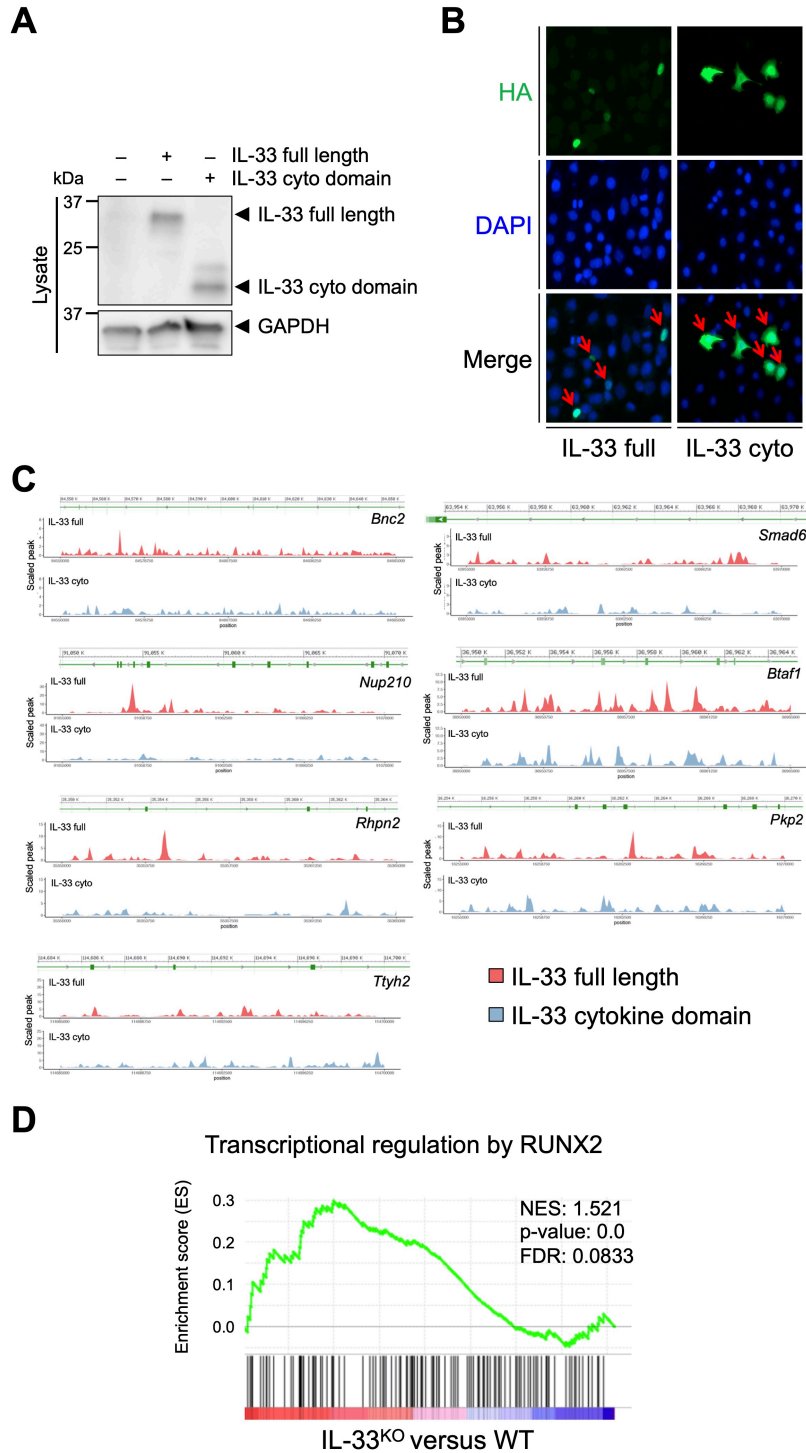
(F) Representative images of IL-33 immunostained DNFB-treated skin and AOM/DSS-treated colon tissues from IL-33^{KO} mice (scale bars: 100 μ m).

Data information: Graphs show mean + SD, NS: not significant, unpaired *t*-test.



Appendix Fig S2. RNA-Seq analysis to identify IL-33 nuclear function.

- (A) The experimental design used to induce chronic skin inflammation with repeated topical DNFB treatment. At the completion of the 22-day treatment period, epidermis samples were collected for RNA-Seq.
- (B) Representative images of IL-33^{KO} and WT mice after 22-day DNFB back skin treatment (scale bar: 1 cm).
- (C) Top 20 differentially expressed genes (DEGs) in DNFB-treated IL-33^{KO} compared with WT epidermis from RNA-Seq.
- (D) Biological pathways highlighted by DEGs from RNA-Seq.
- (E) The enrichment plot of negative regulation of BMP signaling pathway gene set in IL-33^{KO} compared with WT epidermis treated with DNFB.
- (F) Heatmap of negative regulation of TGF- β /BMP signaling pathway gene set in IL-33^{KO} versus WT epidermis after topical treatment with DNFB. This gene list contains several genes (highlighted) that are shared between BMP and TGF- β signaling pathways.
- (G) The enrichment plot of a restricted SMAD protein phosphorylation gene set in IL-33^{KO} compared with WT epidermis treated with DNFB.



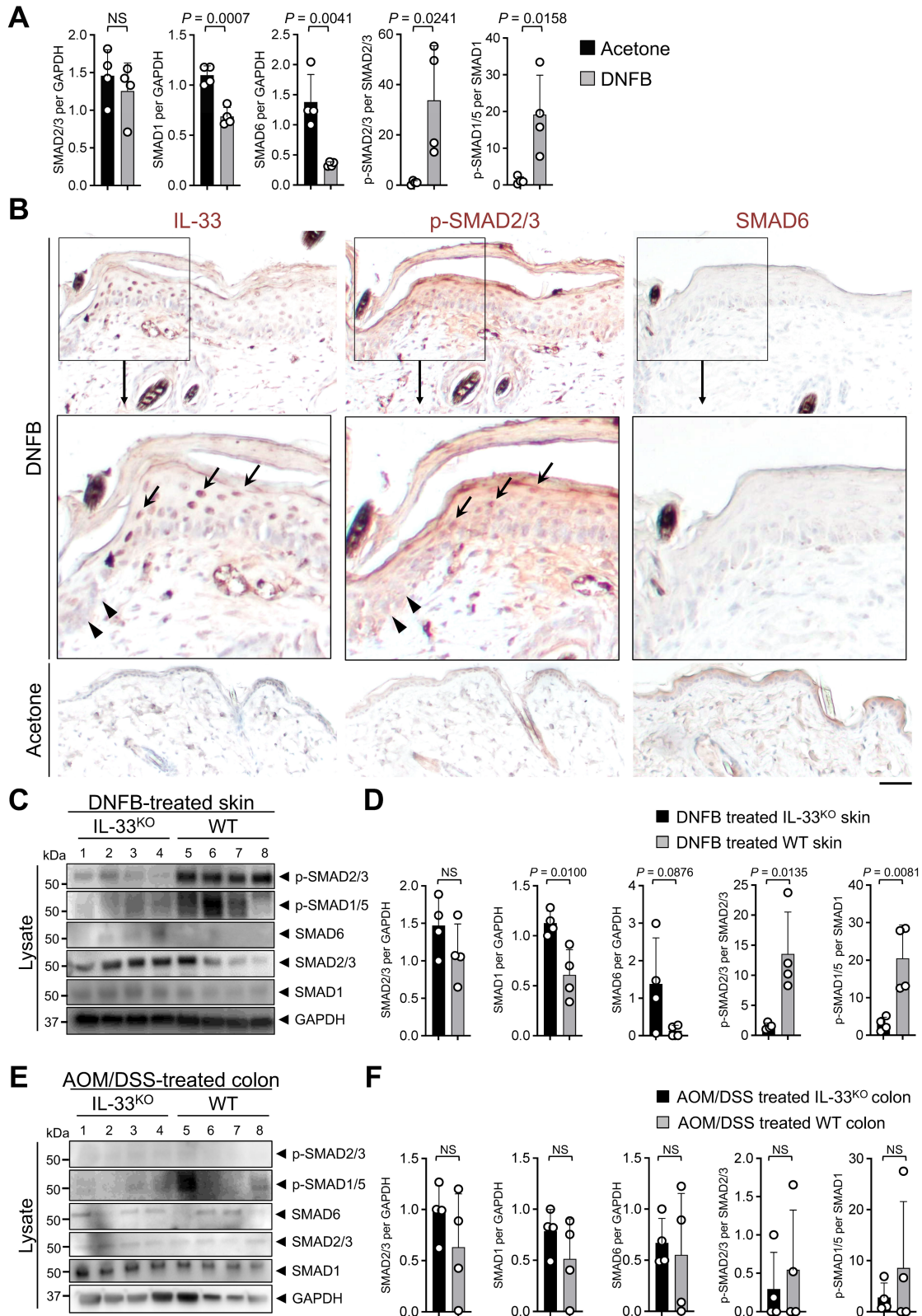
Appendix Fig S3. Integrative analysis of RNA-Seq and ChIP-Seq results.

(A) Expression of IL-33 full length and IL-33 cytokine domain in Pam212 cells. GAPDH is used as the control housekeeping protein.

(B) Representative images for localization of IL-33 expression constructs. Anti-HA antibody marks the IL-33 constructs. Red arrows point to the IL-33-positive cells.

(C) Peak calling analysis of genes identified from the integrative analysis of RNA-Seq and CHIP-Seq results. Genome-browser views of IL-33 full length (full) and IL-33 cytokine domain (cyto) CHIP-Seq signals for *Bnc2*, *Nup210*, *Rhpn2*, *Ttyh2*, *Smad6*, *Btaf1* and *Pkp2* genes.

(D) The enrichment plot of transcriptional regulation by RUNX2 gene set in IL-33^{KO} compared with WT epidermis treated with DNFB from RNA-Seq analysis.



Appendix Fig S4. IL-33 regulates SMAD signaling in inflamed skin but not the colon.

(A) Quantification of protein bands shown in Figure 3A.

(B) Representative images of IL-33, p-SMAD2/3 and SMAD6 IHC on the adjacent sections of DNFB versus acetone-treated mouse skin. Arrows in the insets point to nuclear IL-33 and p-SMAD2/3 stains in the epidermis and arrowheads highlight keratinocytes nuclei that are negative for both IL-33 and p-SMAD2/3 (scale bar: 100 μ m).

(C) Immunoblots for p-SMAD2/3, p-SMAD1/5, SMAD6, SMAD2/3 and SMAD1 proteins in IL-33^{KO} and WT skin after DNFB treatment.

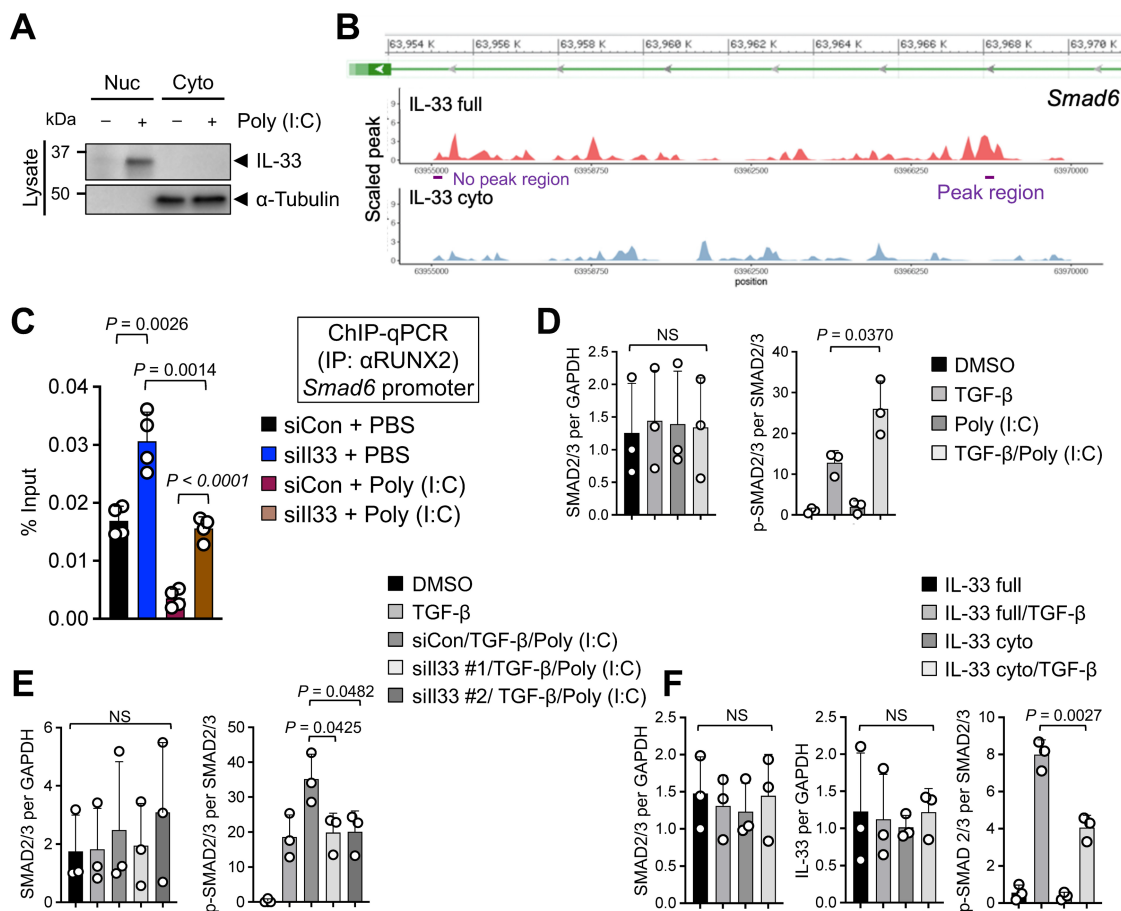
(D) Quantification of protein bands shown in S4C.

(E) Immunoblots for p-SMAD2/3, p-SMAD1/5, SMAD6, SMAD2/3 and SMAD1 proteins in IL-33^{KO} and WT colon after AOM/DSS treatment.

(F) Quantification of protein bands shown in S4E.

Data information: GAPDH is used as the control housekeeping protein, graphs show mean + SD,

NS: not significant, unpaired *t*-test.



Appendix Fig S5. Nuclear IL-33 induced by poly (I:C) binds to the *Smad6* regulatory region.

(A) IL-33 protein levels in nuclear (Nuc) and cytoplasmic (Cyto) fractions of Pam212 cells treated with poly (I:C). Each fraction's lysate was subjected to immunoblot with anti-IL-33 and anti- α -tubulin antibodies.

(B) Peak and no peak regions of *Smad6* regulatory region amplified in ChIP-qPCR assay using an anti-IL-33 antibody.

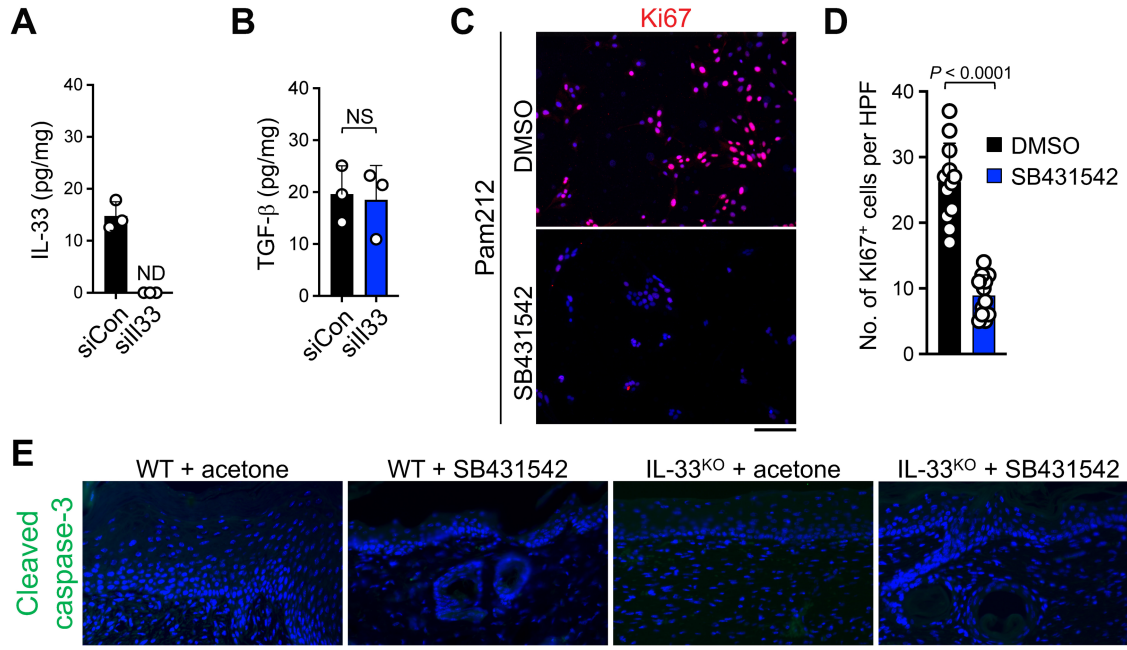
(C) ChIP-qPCR assay for *Smad6* promoter upon induction of endogenous IL-33 with or without sill33 using an anti-RUNX2 antibody. After transfection with sill33 #1 or control siRNA (siCon) for 24 hours, Pam212 cells were treated with poly (I:C) or PBS (carrier control). Cell lysates were subjected to chromatin-immunoprecipitation with anti-RUNX2 antibody and eluted RUNX2-bound chromatin was used for qPCR with *Smad6* promoter primers.

(D) Quantification of protein bands shown in Figure 3D.

(E) Quantification of protein bands shown in Figure 3E.

(F) Quantification of protein bands shown in Figure 3F.

Data information: Graphs show mean + SD, NS: not significant, unpaired *t*-test.



Appendix Fig S6. SB431542 blocks keratinocyte proliferation but does not induce apoptosis.

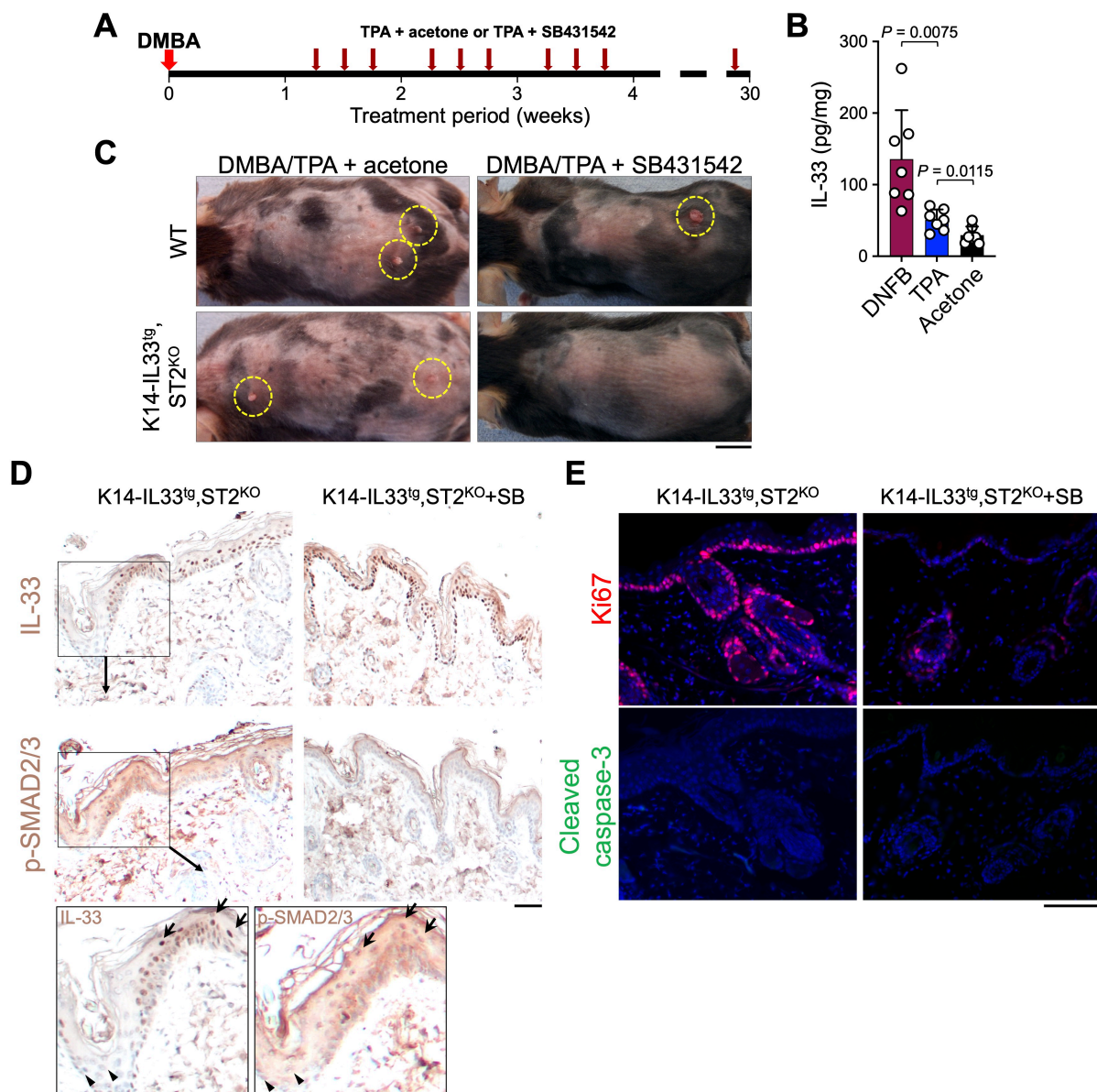
(A and B) Endogenous (A) IL-33 and (B) TGF- β protein levels in Pam212 cell lysate after treatment with sill33 versus siCon. ND: not detected, NS: not significant.

(C) Representative images of Ki67-stained Pam212 cells treated with SB431542 or DMSO (carrier control) for 24 hours.

(D) Quantification of Ki67⁺ Pam212 cells treated with SB431542 versus DMSO (unpaired *t*-test).

(E) Representative images of cleaved caspase-3 immunofluorescence-stained skin tissues shown in Figure 3I.

Data information: Scale bars: 100 μ m.



Appendix Fig S7. Blocking TGF- β /SMAD signaling attenuates nuclear IL-33 induced skin cancer development.

(A) Experimental design for DMBA/TPA skin carcinogenesis protocol in combination with TGF- β /SMAD inhibitor, SB431542, treatment.

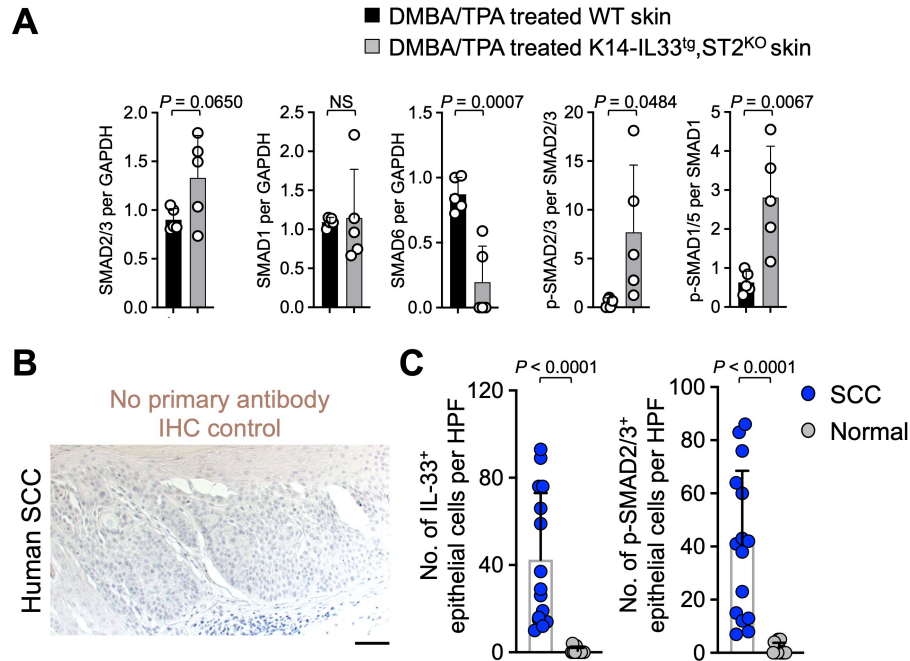
(B) IL-33 protein levels in TPA- and DNFB-treated skin compared with acetone (carrier)-treated controls (n=7 in each group, graph shows mean + SD, unpaired *t*-test).

(C) Representative images of WT and K14-IL33^{tg},ST2^{KO} mice treated with SB431542 or acetone (carrier control) at the completion of DMBA/TPA carcinogenesis protocol (yellow circles highlight the skin tumors).

(D) Representative images of IL-33 and p-SMAD2/3 immunostained adjacent skin sections from SB431542 and acetone-treated K14-IL33^{tg},ST2^{KO} mice that completed DMBA/TPA carcinogenesis protocol. Arrows point to IL-33⁺ and p-SMAD2/3⁺ epidermal keratinocytes. Arrowheads highlight keratinocytes that lack both IL-33 and p-SMAD2/3.

(E) Representative images of Ki67 and cleaved caspase-3 immunofluorescence staining on the adjacent sections of SB431542 and acetone-treated K14-IL33^{tg},ST2^{KO} skin that underwent DMBA/TPA carcinogenesis protocol.

Data information: Scale bars: mouse 1cm, tissue 100 μ m.



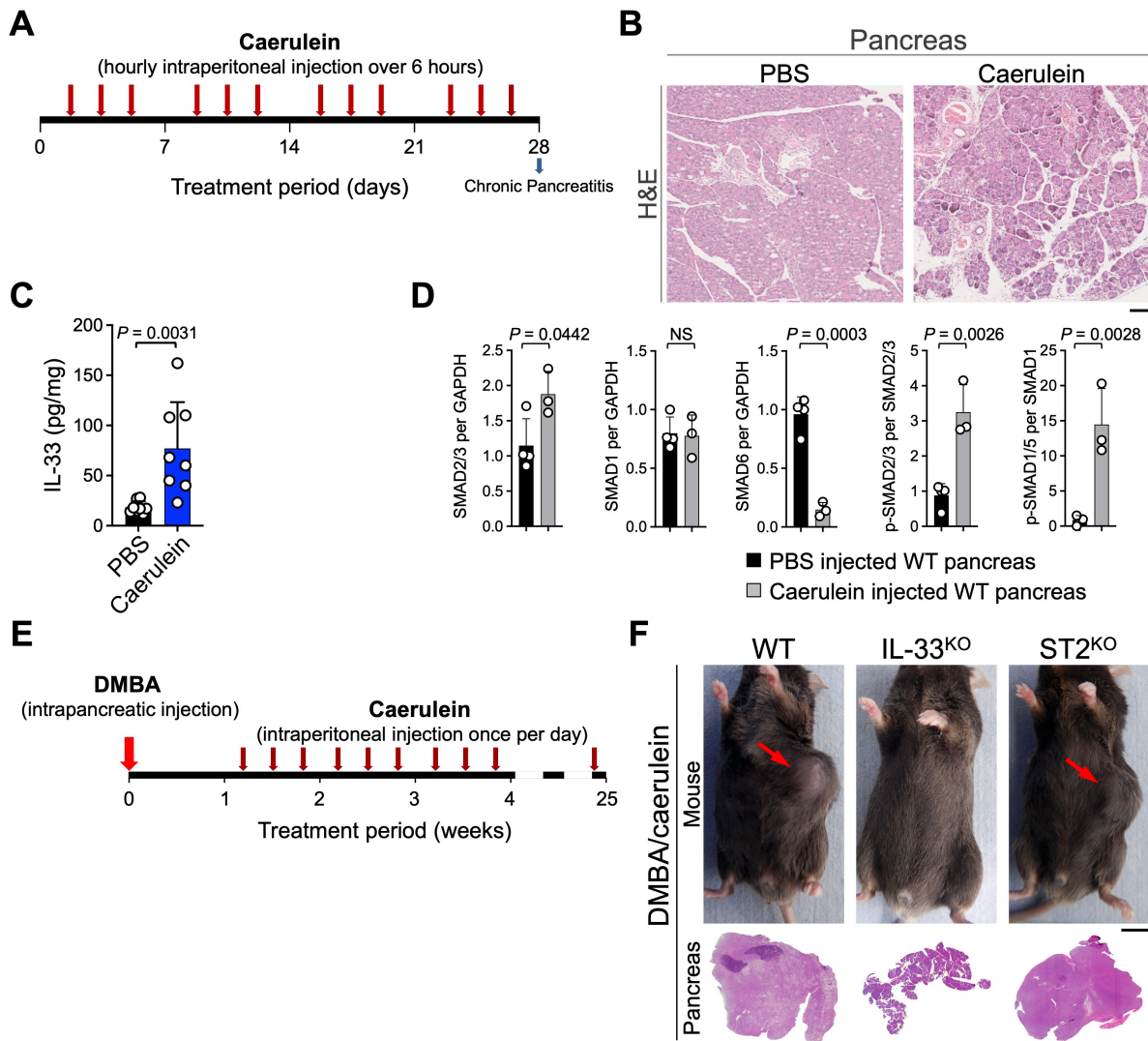
Appendix Fig S8. IL-33 and p-SMAD2/3 are highly expressed in human SCC.

(A) Quantification of protein bands shown in Figure 4I.

(B) Representative image of negative control (no primary antibody) immunostaining on the adjacent tissue section of the human SCC sample shown in Figure 4J (scale bar: 100 μ m).

(C) Quantification of nuclear IL-33⁺ and p-SMAD2/3⁺ epithelial cells per HPF in SCC versus normal human skin. Dots represent cell counts in three randomly selected HPF images per sample across 5 SCC and 5 normal skin samples.

Data information: Graphs show mean + SD, NS: not significant, unpaired *t*-test.



Appendix Fig S9. Nuclear IL-33 promotes pancreatic cancer development in chronic pancreatitis.

- (A) Experimental design for the induction of chronic pancreatitis in mice.
- (B) Representative images of H&E-stained pancreas of WT mice treated with caerulein versus PBS (carrier control) for 4 weeks (scale bar: 100 μ m).
- (C) IL-33 protein levels in caerulein- compared with PBS-treated pancreas.
- (D) Quantification of protein bands shown in Figure 5C.

(E) Experimental design for DMBA/caerulein-induced pancreatic cancer including an intrapancreatic injection with DMBA followed by intraperitoneal caerulein injections once per day, three times a week for 24 weeks.

(F) Representative images of DMBA/caerulein-treated WT, IL-33^{KO} and ST2^{KO} mice and H&E-stained pancreas of WT, IL-33^{KO} and ST2^{KO}. Red arrows point to pancreatic tumor mass under the skin of WT and ST2^{KO} mice. Note the replacement of pancreas with large fibrotic tumors in WT and ST2^{KO} mice (scale bar: 1 cm).

Data information: Graphs show mean + SD, NS: not significant, unpaired *t*-test.

Appendix Tables

Appendix Table S1. List of 203 DEGs from RNA-Seq analysis of IL-33^{KO} versus WT epidermis treated with DNFB.

<u>Gene ID</u>	<u>Gene Name</u>	<u>Gene Description</u>
ENSMUSG00000000184	Ccnd2	cyclin_D2
ENSMUSG00000001510	Dlx3	distal-less_homeobox_3
ENSMUSG00000001655	Hoxc13	homeobox_C13
ENSMUSG00000002057	Foxn1	forkhead_box_N1
ENSMUSG00000003418	St8sia6	ST8_alpha-N-acetyl-neuraminide_alpha-28-sialyltransferase_6
ENSMUSG00000003545	Fosb	FBJ_osteosarcoma_oncogene_B
ENSMUSG00000004552	Ctse	cathepsin_E
ENSMUSG00000005262	Ufd1l	ubiquitin_fusion_degradation_1_like
ENSMUSG00000006345	Ggt1	gamma-glutamyltransferase_1
ENSMUSG00000014846	Tppp3	tubulin_polymerization-promoting_protein_family_member_3
ENSMUSG00000015441	Gzmf	granzyme_F
ENSMUSG00000015619	Gata3	GATA_binding_protein_3
ENSMUSG00000015957	Wnt11	wingless-type_MMTV_integration_site_family_member_11
ENSMUSG00000017588	Krt27	keratin_27
ENSMUSG00000018983	E2f2	E2F_transcription_factor_2
ENSMUSG00000019564	Arid3a	AT_rich_interactive_domain_3A_(BRIGHT-like)
ENSMUSG00000020099	Unc5b	unc-5_homolog_B_(C_elegans)
ENSMUSG00000020216	Jsrp1	junctional_sarcoplasmic_reticulum_protein_1
ENSMUSG00000020473	Aebp1	AE_binding_protein_1
ENSMUSG00000020723	Cacng4	calcium_channel_voltage-dependent_gamma_subunit_4
ENSMUSG00000020732	Rab37	RAB37_member_RAS_oncogene_family
ENSMUSG00000020871	Dlx4	distal-less_homeobox_4
ENSMUSG00000020891	Alox8	arachidonate_8-lipoxygenase
ENSMUSG00000020916	Krt36	keratin_36
ENSMUSG00000021061	Sptb	spectrin_beta_erythrocytic
ENSMUSG00000021250	Fos	FBJ_osteosarcoma_oncogene
ENSMUSG00000021469	Msx2	msh_homeobox_2
ENSMUSG00000022044	Stmn4	stathmin-like_4
ENSMUSG00000022243	Slc45a2	solute_carrier_family_45_member_2
ENSMUSG00000022415	Syng1	synaptogyrin_1
ENSMUSG00000022658	Tagln3	transgelin_3
ENSMUSG00000022871	Fetub	fetuin_beta
ENSMUSG00000022986	Krt75	keratin_75
ENSMUSG00000023034	Nr4a1	nuclear_receptor_subfamily_4_group_A_member_1

ENSMUSG00000023387	Kcnk16	potassium_channel_subfamily_K_member_16
ENSMUSG00000023391	Dlx2	distal-less_homeobox_2
ENSMUSG00000024059	Clip4	CAP-GLY_domain_containing_linker_protein_family_member_4
ENSMUSG00000024190	Dusp1	dual_specificity_phosphatase_1
ENSMUSG00000024232	Bambi	BMP_and_activin_membrane-bound_inhibitor
ENSMUSG00000024353	Mzb1	marginal_zone_B_and_B1_cell-specific_protein_1
ENSMUSG00000024409	Psors1c2	psoriasis_susceptibility_1_candidate_2_(human)
ENSMUSG00000024471	Myot	myotilin
ENSMUSG00000024538	Ppic	peptidylprolyl_isomerase_C
ENSMUSG00000024806	Mlana	melan-A
ENSMUSG00000024810	Il33	interleukin_33
ENSMUSG00000024975	Pdcd4	programmed_cell_death_4
ENSMUSG00000025328	Padi3	peptidyl_arginine_deiminase_type_III
ENSMUSG00000025329	Padi1	peptidyl_arginine_deiminase_type_I
ENSMUSG00000025359	Pmel	premelanosome_protein
ENSMUSG00000025407	Gli1	GLI-Kruppel_family_member_GLI1
ENSMUSG00000025453	Nnt	nicotinamide_nucleotide_transhydrogenase
ENSMUSG00000025461	Cd163l1	CD163_molecule-like_1
ENSMUSG00000026407	Cacna1s	calcium_channel_voltage-dependent_L_type_alpha_1S_subunit
ENSMUSG00000026420	Il24	interleukin_24
ENSMUSG00000026489	Adck3	aarF_domain_containing_kinase_3
ENSMUSG00000026950	Neb	nebulin
ENSMUSG00000027015	Cybrd1	cytochrome_b_reductase_1
ENSMUSG00000027403	Tgm6	transglutaminase_6
ENSMUSG00000027470	Mylk2	myosin_light_polypeptide_kinase_2_skeletal_muscle
ENSMUSG00000027487	Cdk5rap1	CDK5_regulatory_subunit_associated_protein_1
ENSMUSG00000027800	Tm4sf1	transmembrane_4_superfamily_member_1
ENSMUSG00000028111	Ctsk	cathepsin_K
ENSMUSG00000028195	Cyr61	cysteine_rich_protein_61
ENSMUSG00000028358	Zfp618	zinc_finger_protein_618
ENSMUSG00000028487	Bnc2	basonuclin_2
ENSMUSG00000028654	Mycl	v-myc_myelocytomatosis_viral_oncogene_homolog_lung_carcinoma_derived_(avian)
ENSMUSG00000028681	Ptch2	patched_homolog_2
ENSMUSG00000028698	Pik3r3	phosphatidylinositol_3_kinase_regulatory_subunit_polypeptide_3_(p55)
ENSMUSG00000028940	Hes2	hairy_and_enhancer_of_split_2_(Drosophila)
ENSMUSG00000029070	Mxra8	matrix-remodelling_associated_8
ENSMUSG00000029095	Ablim2	actin-binding_LIM_protein_2
ENSMUSG00000029337	Fgf5	fibroblast_growth_factor_5
ENSMUSG00000029380	Cxcl1	chemokine_(C-X-C_motif)_ligand_1

ENSMUSG00000029641	Rasl11a	RAS-like_family_11_member_A
ENSMUSG00000029705	Cux1	cut-like_homeobox_1
ENSMUSG00000030091	Nup210	nucleoporin_210
ENSMUSG00000030108	Slc6a13	solute_carrier_family_6_(neurotransmitter_transporter_GABA)_member_13
ENSMUSG00000030205	Gprc5d	G_protein-coupled_receptor_family_C_group_5_member_D
ENSMUSG00000030409	Dmpk	dystrophia_myotonica-protein_kinase
ENSMUSG00000030494	Rhpn2	rhophilin_Rho_GTPase_binding_protein_2
ENSMUSG00000030523	Trpm1	transient_receptor_potential_cation_channel_subfamily_M_member_1
ENSMUSG00000030592	Ryr1	ryanodine_receptor_1_skeletal_muscle
ENSMUSG00000030717	Nupr1	nuclear_protein_transcription_regulator_1
ENSMUSG00000030739	Myh14	myosin_heavy_polypeptide_14
ENSMUSG00000030905	Crym	crystallin_mu
ENSMUSG00000031963	Bmper	BMP-binding_endothelial_regulator
ENSMUSG00000031995	St14	suppression_of_tumorigenicity_14_(colon_carcinoma)
ENSMUSG00000032053	Pou2af1	POU_domain_class_2_associating_factor_1
ENSMUSG00000032327	Stra6	stimulated_by_retinoic_acid_gene_6
ENSMUSG00000032368	Zic1	zinc_finger_protein_of_the_cerebellum_1
ENSMUSG00000032500	Dclk3	doublecortin-like_kinase_3
ENSMUSG00000032648	Pygm	muscle_glycogen_phosphorylase
ENSMUSG00000032841	Prr5l	proline_rich_5_like
ENSMUSG00000034714	Ttyh2	tweety_homolog_2_(Drosophila)
ENSMUSG00000035385	Ccl2	chemokine_(C-C_motif)_ligand_2
ENSMUSG00000035831	Krt25	keratin_25
ENSMUSG00000036306	Lzts1	leucine_zipper_putative_tumor_suppressor_1
ENSMUSG00000036867	Smad6	SMAD_family_member_6
ENSMUSG00000036923	Stox1	storkhead_box_1
ENSMUSG00000037169	Mycn	v-myc_myelocytomatosis_viral_related_oncogene_neuroblastoma_derived_(avian)
ENSMUSG00000037434	Slc30a1	solute_carrier_family_30_(zinc_transporter)_member_1
ENSMUSG00000037846	Rtkn2	rhotekin_2
ENSMUSG00000037977	6430571L13Rik	RIKEN_cDNA_6430571L13_gene
ENSMUSG00000038580	Sct	secretin
ENSMUSG00000038599	Capn8	calpain_8
ENSMUSG00000039217	Il18	interleukin_18
ENSMUSG00000039323	Igfbp2	insulin-like_growth_factor_binding_protein_2
ENSMUSG00000040565	Btaf1	BTAf1_RNA_polymerase_II_B-TFIID_transcription_factor-associated_(Mot1_homolog_S._cerevisiae)
ENSMUSG00000041120	Nbl1	neuroblastoma_suppression_of_tumorigenicity_1
ENSMUSG00000041911	Dlx1	distal-less_homeobox_1
ENSMUSG00000041957	Pkp2	plakophilin_2

ENSMUSG00000042092	Lce1c	late_cornified_envelope_1C
ENSMUSG00000042109	Csdc2	cold_shock_domain_containing_C2_RNA_binding
ENSMUSG00000042532	Golga7b	golgi_autoantigen_golgin_subfamily_a_7B
ENSMUSG00000043461	Sptssb	serine_palmitoyltransferase_small_subunit_B
ENSMUSG00000044243	Bhlha9	basic_helix-loop-helix_family_member_a9
ENSMUSG00000044430	Klk12	kallikrein_related-peptidase_12
ENSMUSG00000044594	Serpib3a	serine_(or_cysteine)_peptidase_inhibitor_clade_B_(ovalbumin)_member_3A
ENSMUSG00000045005	Fzd5	frizzled_homolog_5_(Drosophila)
ENSMUSG00000046676	Lce1l	late_cornified_envelope_1L
ENSMUSG00000046997	Spsb4	splA/ryanodine_receptor_domain_and_SOCS_box_containing_4
ENSMUSG00000047419	Cmya5	cardiomyopathy_associated_5
ENSMUSG00000047420	Fam180a	family_with_sequence_similarity_180_member_A
ENSMUSG00000047632	Fgfbp3	fibroblast_growth_factor_binding_protein_3
ENSMUSG00000048450	Msx1	msh_homeobox_1
ENSMUSG00000048582	Gja3	gap_junction_protein_alpha_3
ENSMUSG00000051586	Mical3	microtubule_associated_monooxygenase_calponin_and_LIM_domain_containing_3
ENSMUSG00000051879	Krt71	keratin_71
ENSMUSG00000052302	Tbc1d30	TBC1_domain_family_member_30
ENSMUSG00000052415	Tchh	trichohyalin
ENSMUSG00000052512	Nav2	neuron_navigator_2
ENSMUSG00000053414	Hunk	hormonally_upregulated_Neu-associated_kinase
ENSMUSG00000053897	Slc39a8	solute_carrier_family_39_(metal_ion_transporter)_member_8
ENSMUSG00000054083	Capn12	calpain_12
ENSMUSG00000054196	Cthrc1	collagen_triple_helix_repeat_containing_1
ENSMUSG00000055194	Actbl2	actin_beta-like_2
ENSMUSG00000055632	Hmcn2	hemicentin_2
ENSMUSG00000055937	Krt28	keratin_28
ENSMUSG00000056270	Prr9	proline_rich_9
ENSMUSG00000056605	Krt72	keratin_72
ENSMUSG00000057137	Tmem140	transmembrane_protein_140
ENSMUSG00000058914	C1qtnf3	C1q_and_tumor_necrosis_factor_related_protein_3
ENSMUSG00000059493	Nhs	Nance-Horan_syndrome_(human)
ENSMUSG00000059921	Unc5c	unc-5_homolog_C_(C._elegans)
ENSMUSG00000059970	Hspa2	heat_shock_protein_2
ENSMUSG00000066677	Pydc3	pyrin_domain_containing_3
ENSMUSG00000066975	Cryba4	crystallin_beta_A4
ENSMUSG00000067149	Igj	immunoglobulin_joining_chain
ENSMUSG00000068874	Selenbp1	selenium_binding_protein_1
ENSMUSG00000070990	Foxe1	forkhead_box_E1

ENSMUSG00000072844	G530011O06Rik	RIKEN_cDNA_G530011O06_gene
ENSMUSG00000073413	Ly6g6d	lymphocyte_antigen_6_complex_locus_G6D
ENSMUSG00000073643	Wdfy1	WD_repeat_and_FYVE_domain_containing_1
ENSMUSG00000073791	Efcab7	EF-hand_calcium_binding_domain_7
ENSMUSG00000074037	Mc1r	melanocortin_1_receptor
ENSMUSG00000074093	Svip	small_VCP/p97-interacting_protein
ENSMUSG00000074206	Adh6b	alcohol_dehydrogenase_6B_(class_V)
ENSMUSG00000074445	Sprr2a3	small_proline-rich_protein_2A3
ENSMUSG00000075570	Krt26	keratin_26
ENSMUSG00000076508	Igkv17-127	immunoglobulin_kappa_variable_17-127
ENSMUSG00000076514	Igkv17-121	immunoglobulin_kappa_variable_17-121
ENSMUSG00000076523	Igkv15-103	immunoglobulin_kappa_chain_variable_15-103
ENSMUSG00000076526	Igkv12-98	immunoglobulin_kappa_variable_12-98
ENSMUSG00000076563	Igkv5-48	immunoglobulin_kappa_variable_5-48
ENSMUSG00000076564	Igkv12-46	immunoglobulin_kappa_variable_12-46
ENSMUSG00000076569	Igkv5-39	immunoglobulin_kappa_variable_5-39
ENSMUSG00000076577	Igkv8-30	immunoglobulin_kappa_chain_variable_8-30
ENSMUSG00000076609	Igkc	immunoglobulin_kappa_constant
ENSMUSG00000076613	Ighg2b	immunoglobulin_heavy_constant_gamma_2B
ENSMUSG00000076672	Ighv3-6	immunoglobulin_heavy_variable_3-6
ENSMUSG00000076674	Ighv3-8	immunoglobulin_heavy_variable_V3-8
ENSMUSG00000076934	Iglv1	immunoglobulin_lambda_variable_1
ENSMUSG00000076937	Iglc2	immunoglobulin_lambda_constant_2
ENSMUSG00000078657	Crnn	cornulin
ENSMUSG00000084228	Gm8080	predicted_gene_8080
ENSMUSG00000085645	Hoxb5os	homeobox_B5_and_homeobox_B6_opposite_strand
ENSMUSG00000092341	Malat1	metastasis_associated_lung_adenocarcinoma_transcript_1_(non-coding_RNA)
ENSMUSG00000092572	Serpib10	serine_(or_cysteine)_peptidase_inhibitor_clade_B_(ovalbumin)_member_10
ENSMUSG00000093861	Igkv1-110	immunoglobulin_kappa_variable_1-110
ENSMUSG00000094335	Igkv1-117	immunoglobulin_kappa_variable_1-117
ENSMUSG00000094420	Igkv10-96	immunoglobulin_kappa_variable_10-96
ENSMUSG00000094546	Ighv1-26	immunoglobulin_heavy_variable_1-26
ENSMUSG00000094724	Rnaset2b	ribonuclease_T2B
ENSMUSG00000094797	Igkv6-15	immunoglobulin_kappa_variable_6-15
ENSMUSG00000094930	Igkv6-25	immunoglobulin_kappa_chain_variable_6-25
ENSMUSG00000095079	Igha	immunoglobulin_heavy_constant_alpha
ENSMUSG00000095351	Igkv3-2	immunoglobulin_kappa_variable_3-2
ENSMUSG00000095571	Ighv5-17	immunoglobulin_heavy_variable_5-17
ENSMUSG00000095630	Igkv6-23	immunoglobulin_kappa_variable_6-23

ENSMUSG00000095687	Rnaset2a	ribonuclease_T2A
ENSMUSG00000095700	Ighv10-3	immunoglobulin_heavy_variable_V10-3
ENSMUSG00000095870	Lce1k	late_cornified_envelope_1K
ENSMUSG00000095930	Nim1k	NIM1_serine/threonine_protein_kinase
ENSMUSG00000096255	Dynlt1b	dynein_light_chain_Tctex-type_1B
ENSMUSG00000096336	Igkv1-135	immunoglobulin_kappa_variable_1-135
ENSMUSG00000096422	Igkv12-44	immunoglobulin_kappa_variable_12-44
ENSMUSG00000096459	Ighv9-3	immunoglobulin_heavy_variable_V9-3
ENSMUSG00000096715	Igkv3-4	immunoglobulin_kappa_variable_3-4
ENSMUSG00000096768	Erdr1	erythroid_differentiation_regulator_1
ENSMUSG00000096780	Tmem181b-ps	transmembrane_protein_181B_pseudogene
ENSMUSG00000096862	Gm13301	predicted_gene_13301
ENSMUSG00000097296	Gm26532	predicted_gene_26532
ENSMUSG00000101026	RP23-230O9.7	RIKEN_cDNA_D730001G18_gene

Appendix Table S2. Antibodies, staining kits and primers information.

<u>Western blotting Antibodies</u>	<u>Clone</u>	<u>Company</u>
<i>Primary antibodies</i>		
p-SMAD2/3	D27F4	Cell Signaling Technology, Danvers, MA
p-SMAD1/5	41D10	Cell Signaling Technology
RUNX2	D1L7F	Cell Signaling Technology
GAPDH	D16H11	Cell Signaling Technology
Anti-mouse IL-33	Polyclonal	R&D Systems, Minneapolis, MN
SMAD2/3	Polyclonal	R&D Systems
SMAD6	Polyclonal	NOVUS biologicals, Centennial, CO
SMAD1	EP565Y	Abcam, Cambridge, UK
HA	16B12	Biolegend, San Diego, CA
<i>Secondary antibodies</i>		
	<u>Cat #</u>	<u>Company</u>
Peroxidase Goat Anti-Mouse IgG	115-035-003	Jackson ImmunoResearch, West Grove, PA
Peroxidase Goat Anti-Rabbit IgG	111-035-003	Jackson ImmunoResearch
Peroxidase Bovine Anti-Goat IgG	805-035-180	Jackson ImmunoResearch
<i>siRNA</i>		
	<u>Cat #</u>	<u>Company</u>
sill33 #1	SI00870443	QIAGEN, Hilden, Germany
sill33 #2	SI00870450	QIAGEN
siCon	1022076	QIAGEN
<i>Immunostaining antibodies</i>		
	<u>Clone</u>	<u>Company</u>
IL-33 (mouse)	Nessy-1	ENZO, Farmingdale, NY
IL-33 (human)	Polyclonal	Sigma, St. Louis, MO
p-SMAD2/3 (mouse and human)	D27F4	Cell Signaling Technology
<i>Staining kits</i>		
	<u>Cat #</u>	<u>Company</u>
Antigen unmasking solution	H3300	Vector Laboratories, Burlingame, CA
VECTASTAIN Elite ABC universal Kit	PK6200	Vector Laboratories
ImmPACT DAB chromogen staining kit	SK-4105	Vector Laboratories
<i>Immunofluorescence staining Antibodies</i>		
	<u>Clone</u>	<u>Company</u>
Ki67	Polyclonal	Abcam
Cleaved caspase-3 (Asp 175)	5A1E	Cell Signaling Technology
<i>Secondary antibodies</i>		
	<u>Cat #</u>	<u>Company</u>
Goat anti-Mouse IgG, Alexa Fluor 488 conjugate	A32723	Thermo Fisher Scientific, Waltham, MA
Goat anti-Rabbit IgG, Alexa Fluor 647 conjugate	A32733	Thermo Fisher Scientific

qPCR primers***Taqman****Il33***Cat #**Mm.PT.58.
12022572**Company**Integrated DNA Technologies, Coralville,
Iowa*Gapdh*

Mm.PT.39a.1

Integrated DNA Technologies

SYBR green*Smad6*

forward: GCAACCCCTACCACTTCAGC

reverse: GTGGCTTGTACTGGTCAGGAG

Gapdh

forward: AATGTGTCCGTCGTGGATCTGA

reverse: GATGCCTGCTTCACCACCTTCT

Smad6 promoter

forward: GGACTGACTCTAAAGTGCTATGCGC

reverse: ACAGTGCCCGCGACTCACTCTCAAG

Smad6 no peak

forward: GTTCAGATGATGTGGCAGAA

reverse: CTTTCTAAGCCCTGGGACCCT

Smad6 peak

forward: CTTGGCAATCCTCAGAGAAG

reverse: ATGAGTGGATTACATAGTCAG

PCR primers for mouse genotyping***Gene name****IL-33*

forward: GAGAGATCAAATGAGGCC

forward mutant: GGTCGCTACCATTACCAG

reverse: GCTGGAGACCAGACTTGT

ST2

forward wild-type: GAAGAGGGCTTCACTCTGTATC

reverse wild-type: GGAGGAGGAGGAGTTGTTAAAG

forward mutant: GATCTCCTGTCATCTCACCTTG

reverse mutant: GCCAACGCTATGTCCTGATA

K14-IL33

forward: GGAGGGGGCAAAGTTTTTCAGGGTG

reverse: TTTGCAAGGCGGGACCAGGG